

UNCLASSIFIED

AD 295 732

*Reproduced
by the*

**ARMED SERVICES TECHNICAL INFORMATION AGENCY
ARLINGTON HALL STATION
ARLINGTON 12, VIRGINIA**



UNCLASSIFIED

NOTICE: When government or other drawings, specifications or other data are used for any purpose other than in connection with a definitely related government procurement operation, the U. S. Government thereby incurs no responsibility, nor any obligation whatsoever; and the fact that the Government may have formulated, furnished, or in any way supplied the said drawings, specifications, or other data is not to be regarded by implication or otherwise as in any manner licensing the holder or any other person or corporation, or conveying any rights or permission to manufacture, use or sell any patented invention that may in any way be related thereto.

63-2-3

CATALOG NO. ASTIA
CATALOG NO. 295732
A-AUG-1963

295732

Unclassified

INTERIM DEVELOPMENT REPORT

For

THE DEVELOPMENT OF GAS LUBRICATED BEARINGS FOR USE IN BLOWER MOTORS

This report covers the period 7 June 1962 to 7 December 1962



ROTRON MANUFACTURING CO.

Woodstock, N. Y.

ASTIA

FEB 8 1963

RECORDED

ASTIA

**NAVY DEPARTMENT BUREAU OF SHIPS ELECTRONICS DIVISION
CONTRACT NUMBER NOber-87522**

Unclassified

Unclassified

INTERIM DEVELOPMENT REPORT

For

THE DEVELOPMENT OF GAS LUBRICATED BEARINGS FOR USE IN BLOWER MOTORS

This report covers the period 7 June 1962 to 7 December 1962



ROTRON MANUFACTURING CO.

Woodstock, N. Y.

**NAVY DEPARTMENT BUREAU OF SHIPS ELECTRONICS DIVISION
CONTRACT NUMBER Nober-87522**

Unclassified

ABSTRACT

Design characteristics of a gas bearing blower motor to meet the requirements of specification MIL-B-21399 and Buships drawing RE-46-C-2105 are presented, utilizing the techniques outlined in a design manual which is being prepared to fulfill the requirements of Contract NObsr 87522.

Calculations show that a plain journal bearing 0.420" diameter by 1.25" long with a diametral clearance of 0.0003" - 0.0004" will provide stable operation at the blower speed, and will permit operation at 10 g's and 55 cps without gas film rupture. Special attention is given to the effect of magnetic loads placed on the bearing by the motor, since such loads are significant in a motor of this size (1-13/16" lamination O.D.).

Other design features, including the methods of shielding the bearing from contamination, and the method of balancing gravity and magnetic loads are presented. Construction of blower motors as described in this report is proceeding.

TABLE OF CONTENTS

	Page No.
I. Purpose	1
II. General Factual Data	
A. Personnel	2
B. References	2 - 4
C. Measurement Procedures	5
III. Detailed Factual Data	
A. Theoretical Design Curves	8 - 17
B. Test Rig Evaluations	17 - 19
C. Gas Bearing Blower Motor	19 - 24
D. Project Performance and Schedule	24 - 26
IV. Conclusions	
A. Future Work	27

LIST OF ILLUSTRATIONS

Figure	Title	Page No.
1	Schematic of Gas Bearing Test Rig	5
2	Schematic of Capacitive Probe Locations	6
3	Journal Bearing Test Rig for 29 Frame Motor	7
4	1/S Plotted Against Eccentricity Ratio for $\Lambda \rightarrow 0$	10
5	Bearing Radial Load Capacity (Plain Journal Bearing)	11
6	Induction Motor Magnetic Force	14
7	Moment Capacity of Full Journal Bearings (Ausman, Reference 5)	15
8	Maximum Moment Angle δ	16

Figure	Title	Page No.
9	29 Frame Size Test Rotor	18
10	29 Frame Blower Motor Design	20
11	Photograph of First Development Prototype Unit	21
12	29 Frame Motor Performance	22
13	Blower Aerodynamic Performance	23
14	Project Performance and Schedule	25

I. PURPOSE

The purpose of the work described in this report is to develop gas lubricated journal and thrust bearings for use in blower motors. The specific goals to be accomplished are:

1. Establishment of theoretical design curves that can be used for the design of gas lubricated bearings suitable for use in the motors of cooling devices delivering air between 10 and 500 cfm.
2. Design and fabrication of a gas lubricated blower motor meeting the requirements of Military Specification MIL-B-21399 and Bureau of Ships Drawing RE-46-C-2105.
3. Demonstration of design capability through performance and qualification tests on three (3) blower units.
4. Delivery to the Bureau of Ships of six gas-bearing blower motors and one set of detailed manufacturing drawings.

To accomplish these goals the program has been broken down into four phases as depicted on the chart on Page 25.

In the first phase bearing design curves will be established using available theoretical data. Wherever possible the design curves will be checked by experimental data.

During the second phase an actual gas-bearing blower motor in the 20 cfm range will be designed and fabricated. Aerodynamic and electrical performance characteristics will be established prior to beginning phase three qualification testing. In the final phase of the program six gas bearing blower units and the associated drawings will be shipped to the Bureau of Ships for further evaluation.

II. GENERAL FACTUAL DATA

A. Personnel

The work presented in this report is being conducted at the Rotron Manufacturing Company with Mr. D. S. Wilson acting as project engineer. Mr. D. D. Fuller (Professor, Columbia University) is serving in the capacity of gas bearing consultant and is responsible for establishment of the theoretical design curves. Electrical design is under the cognizance of the Chief Electrical Engineer, Mr. J. Ebbs, with Mr. B. Larys of the Rotron Research Corporation acting as electrical consultant. The mechanical design is under the cognizance of Mr. D. Harris, the Chief Designer. Mr. R. East is acting as project technician for this program. The accumulated hours spent during this report period by the above personnel are summarized as follows:

D. S. Wilson	- 435-1/2
D. D. Fuller	- 75-1/2
J. Ebbs	- 11
B. Larys	- 40
D. Harris	- 15
R. East	- 230

B. References

1. Drescher, H., "Air Lubricated Bearings, "The Engineers' Digest, Vol. 15, March 1954, pp. 103-107. Abstract from Zeit, V.D.I., Vol. 95, Dec. 11, 1953, pp. 1182-1190.
2. Ford, G. W. K., Harris, D. M., and Pantall, D., "Principles and Applications of Hydrodynamic-Type Gas Bearings, "Proceedings of The Institution of Mechanical Engineers, Vol. 171, No. 2, 1957, pp. 93-113. Discussion, pp. 113-128.
3. Cole, J. A., and Kerr, J., "Observations on the Performance of Air-Lubricated Bearings," Proceedings, Conference on Lubrication and Wear, London, 1957, pp. 164-170.
4. Harrison, W. J., "The Hydrodynamical Theory of Lubrication with Special Reference to Air as a Lubricant," Trans. Cambridge Phil. Soc., Vol. 22, 1912-1923, pp. 39-54.
5. Ausman, J. S., "Theory and Design of Self-Acting, Gas-Lubricated Journal Bearings Including Misalignment Effects," Proceedings, First International Symposium on Gas-Lubricated Bearings, October 1959, pp. 161-192. Superintendent of Documents, U. S. Government Printing Office, Washington 25, D. C., ACR-49.

6. Pantall, D., and Robinson, C. H., "Gas-Lubricated Bearings in Nuclear Engineering," Nuclear Engineering, Feb. 1959, pp. 53-58.
7. Burgdorfer, A., "The Influence of the Molecular Mean Free Path on the Performance of Hydrodynamic Gas-Lubricated Bearings," Trans. A.S.M.E., Journal of Basic Engrg. March 1959, pp. 94-100.
8. Wildmann, M., "Experiments on Gas-Lubricated Journal Bearings," A.S.M.E. Paper No. 56-Lub-8.
9. Fuller, D. D., "Theory and Practice of Lubrication for Engineers", John Wiley and Sons, New York 1956. 432 pages.
10. Elrod, H. G., Jr., and A. Burgdorfer, "Refinements of the Theory of the Infinitely-Long, Self-Acting, Gas-Lubricated Journal Bearing", Proceedings, First International Symposium on Gas-Lubricated Bearings, October, 1959, pp. 93-118. Superintendent of Documents, U. S. Government Printing Office, Washington 25, D. C., ACR-49.
11. Gross, W. A., "Gas Film Lubrication", P. 238. John Wiley and Sons, Inc., New York, 1962. 413 pages.
12. Elrod, H. G., Jr., and S. B. Malanoski, "Theory and Design Data for Continuous-Film, Self-Acting Journal Bearings of Finite Length", Report I-A 2049-13 November 1960, The Franklin Institute Laboratories for Research and Development.
13. Elrod, H. G., Jr., and S. B. Malanoski, "Theory and Design Data for Continuous Film, Self-Acting Journal Bearings of Finite Length, (Supplement to Report I-A 2049-13)" Report I-A2049-17 June 1962, The Franklin Institute Laboratories for Research and Development.
14. Raimondi, A. A., "A Numerical Solution for the Gas Lubricated Full Journal Bearing of Finite Length", Transactions Am. Soc. of Lubrication Engineers, Vol. IV April 1961, pp. 131-155.
15. Hays, D. F., "A Variational Approach to Lubrication Problems and the Solution of the Finite Journal Bearing," Trans. ASME, Vol. 81, No. 1, Mar. 1959, pp. 13-23.
16. Iwasaki, H., "Measurement of Viscosities of Gases at High Pressure, Part I," Sci. Repts. Research Insts. Tohoku Univ., Ser. A, 3, pp. 247-257.
17. Kestin, J., and K. Pilarczyk, "Measurement of the Viscosity of Five Gases at Elevated Pressures by the Oscillating Disk Method," Trans. ASME, Vol. 76, pp. 987-999.

18. Ausman, J. S. "Theory and Design of Self-Acting Gas-Lubricated Journal Bearings Including Misalignment Effects" Proceedings, First International Symposium on Gas-Lubricated Bearings, October, 1959, pp. 161-192. Superintendent of Documents, U. S. Government Printing Office, Washington 25, D. C., ACR-49.
19. Smith, M. I. and D. D. Fuller, "Journal-Bearing Operation at Superlaminar Speeds", Trans. ASME, Vol. 78, April, 1956, pp. 469-474.
20. Sternlicht, B., and R. C. Elwell, "Synchronous Whirl in Plain Journal Bearings" A.S.M.E. Paper Preprint, 62-Lubs-19, 11 pages.
21. Fuller, D. D., "General Review of Gas-Bearing Technology", Proceedings, First International Symposium on Gas-Lubricated Bearings, October, 1959. pp. 1 - 29. Superintendent of Documents, U. S. Government Printing Offices, Washington, D. C., ACR-49
22. Fischer, G. K., J. L. Cherubim, and D. D. Fuller, "Some Instabilities and Operating Characteristics of High-Speed, Gas-Lubricated Journal Bearings", ASME Paper No. 58-A-231.
23. Fischer, G. K., J. L. Cherubim, and O. Decker, "Some Static and Dynamic Characteristics of High-Speed Shaft Systems Operating with Gas-Lubricated Bearings", Proceedings, First International Symposium on Gas-Lubricated Bearings, October 1959. pp. 383-417. Superintendent of Documents, U. S. Government Printing Office, Washington 25, D. C., ACR-49.
24. Hagg, A. C., "The Influence of Oil-Film Journal Bearings on the Stability of Rotating Machines", Trans. A.S.M.E., J1. Applied Mechanics, Vol. 68, 1946, pp. A 211-A 220; Discussion Vol. 69, Mar. 1947, pp. A 77-A 78.
25. Poritsky, H., "A Contribution to the Theory of Oil Whip," Trans. A.S.M.E. Vol. 75, 1953, pp. 1153-1151.
26. Boeker, G. F., and Sternlicht, B., "Investigation of Translatory Fluid Whirl in Vertical Machines," Trans. A.S.M.E., Vol. 78, 1956, pp. 13-19.
27. Bowden and Tabor, "The Friction and Lubrication of Solids", Oxford University Press, London, 1954.
28. Burwell, J. T., "Mechanical Wear", ASM, 1950.
29. First Interim Development Report 7 September 1962. BuShips Contract NObsr 87522, Rotron Manufacturing Company, Inc.

C. Measurement Procedures

Initial evaluations were conducted on a test rig utilizing a 31 frame size motor as described in Reference 29. A second rig has been fabricated as depicted on Figure 1 to accept the 29 frame size motor (1-13/16" O.D.) which is representative of the final motor size. The stationary shaft of this rig is supported at either end with close piloted end caps. Removal of one end cap permits operation as a cantilever supported shaft design. The stationary shaft sleeve is secured to the shaft with epoxy to permit removal for replacement of the sleeve when required. The rotor can be operated as a motor or driven by air with two tangential air jets. This configuration permits bearing performance evaluations with or without electrical loads. Radial loading is accomplished by the use of ball bearings mounted on the rotor O.D.

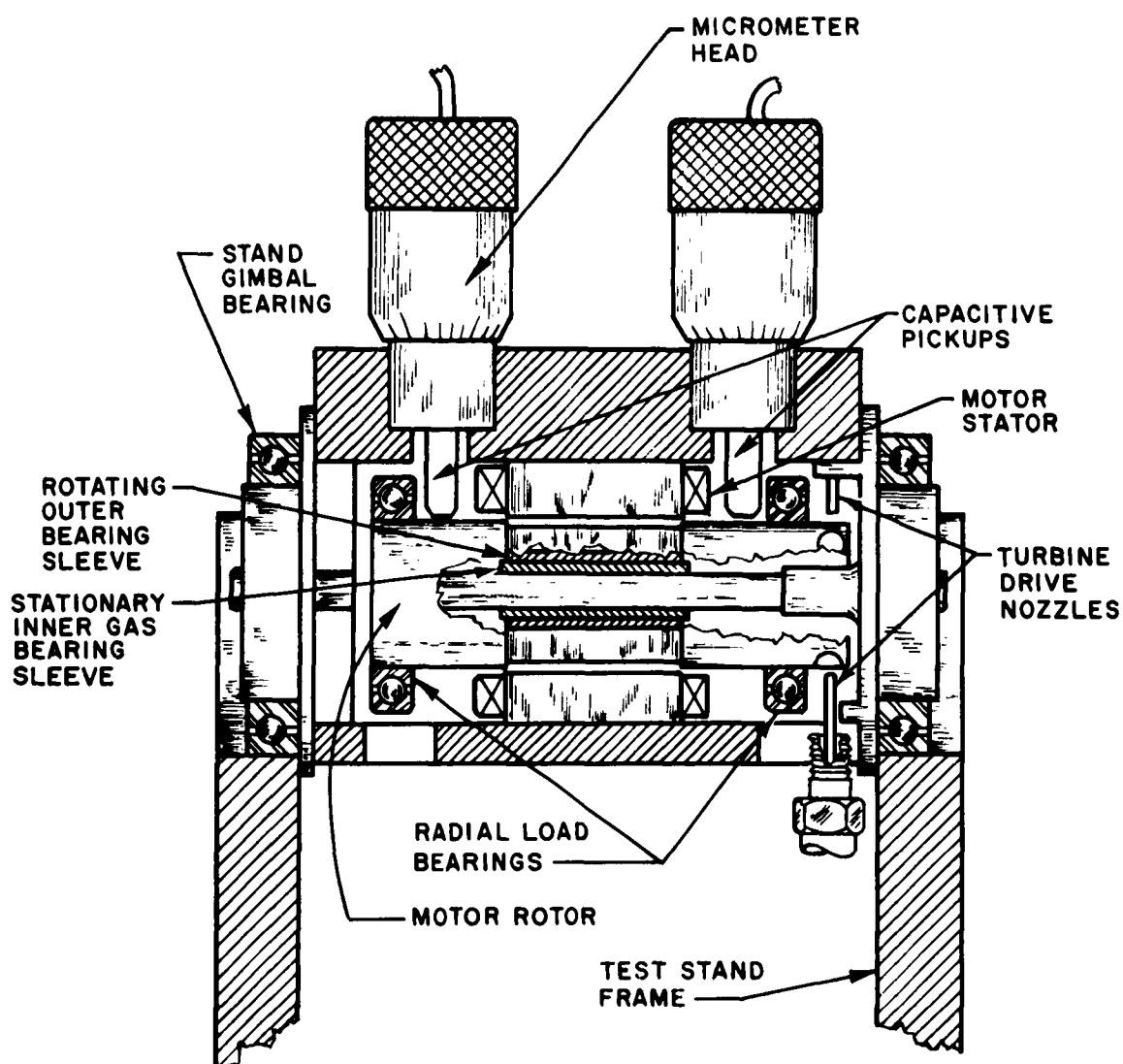


Fig. 1—Schematic of Gas Bearing Test Rig

The rig is instrumented to permit measurement of the dynamic position of the motor rotor while supported on a bearing gas film through the use of a proximity meter and capacitance probes. This type of measuring system, described in Reference 29, functions on the principle of recording capacitance change of the air gap between probe and rotor. Four probes are utilized to monitor rotor movement to permit observation of shaft position in two planes (X, Y) at each end. A polar plot of the rotor center locus at either end of the rotor can be made by applying the output of the X and Y position probes to the horizontal and vertical inputs of a standard oscilloscope (Figure 2).

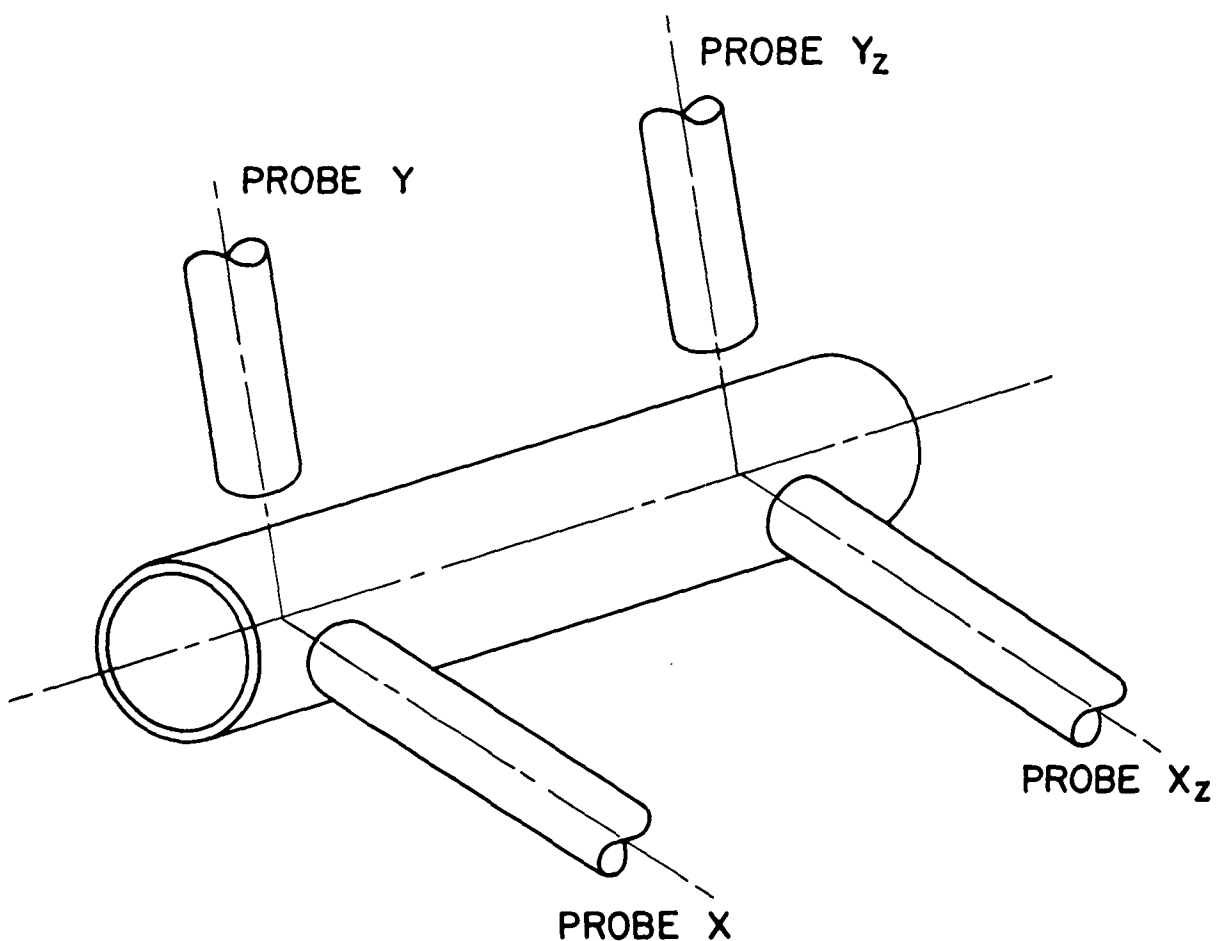


Fig. 2—Schematic of Capacitive Probe Locations

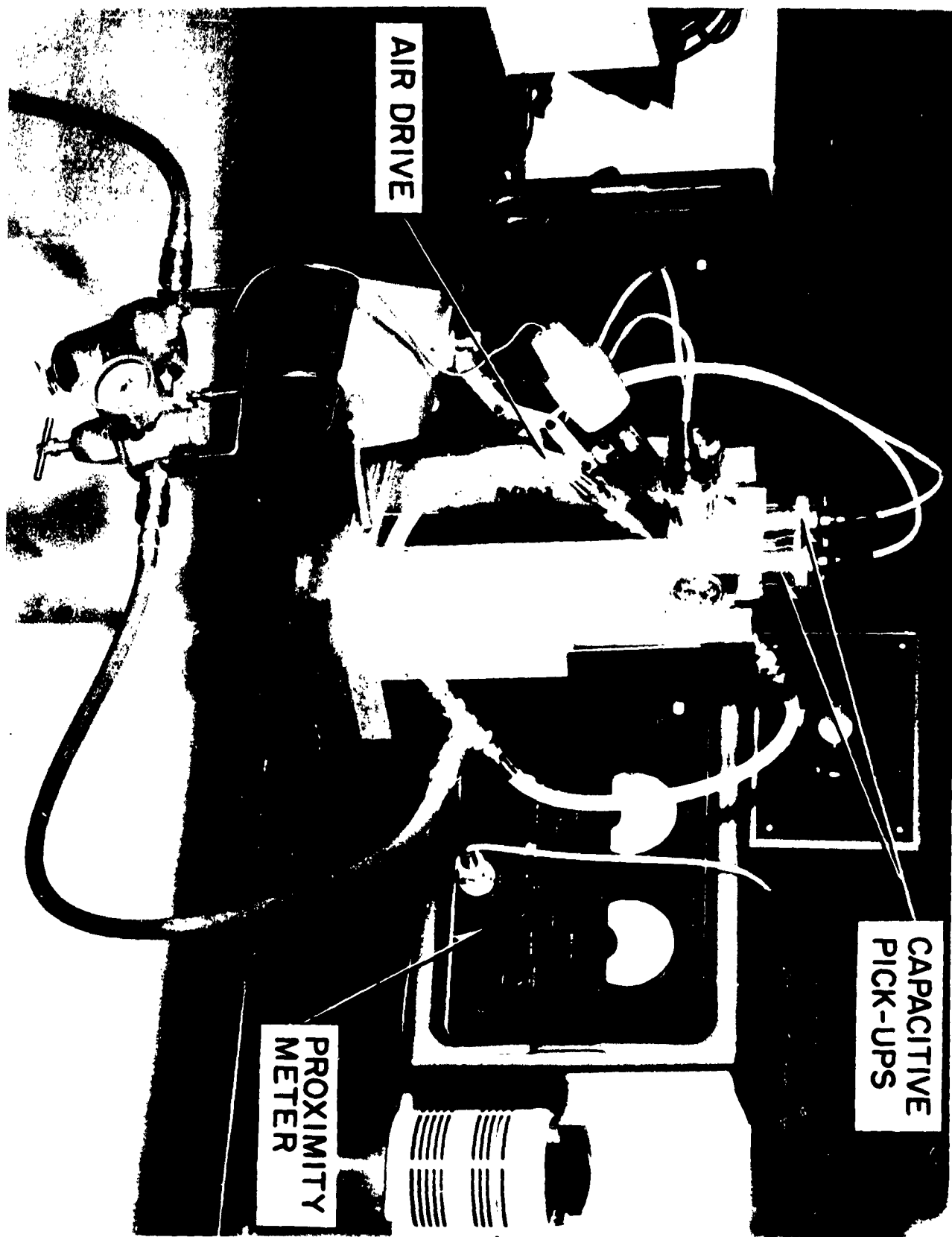


Fig. 3—Journal Bearing Test Rig

III. DETAILED FACTUAL DATA

A. Theoretical Design Curves

A Design Manual is presently being prepared for the purpose of presenting theoretical design curves for use in designing gas bearings for blower motors. Curves and data have been completed for the determination of Journal Bearing Load Capabilities using References 8 through 15, Attitude Angle Determination using References 12, 14, and 19 and Forces Due to Rotating Unbalance, References 20, 21, 22 and 23. Design curves and analytical data for the determination of Half Frequency Whirl and Gas Thrust Bearing Characteristics are in progress.

The use of the Design Manual can best be illustrated by considering the bearing being utilized in the blower motor for this program. This bearing has the following physical characteristics:

Symbol	Description	Magnitude and Dimension
(l)	Bearing Length:	1.250 inch
(d)	Bearing Bore Diameter:	.420 inch
(l/d)	l/d ratio:	1.250/.420 = 2.98
(N)	Rotor Speed:	3300 rpm Maximum
(ω)	Angular Velocity:	$\frac{2\pi}{60} \times 3300 = 345.6$ radians/sec.
(μ)	Gas Viscosity (air at 122°F):	2.86×10^{-9} lb. sec./in. ²
(P _a)	Ambient Pressure:	14.7 psia
(c)	Max. Radial Bearing Clearance:	.00020 inch
(r)	Bearing Radius:	.210 inch
(Λ)	Bearing Compressibility No.	$\frac{6\mu\omega}{P_a} \left(\frac{r}{c}\right)^2$

$$\Lambda = \frac{6(2.86 \times 10^{-9}) \times 345.6}{14.7} \left(\frac{.210}{.0002}\right)^2$$

$$\Lambda = 0.44$$

Due to the low compressibility number (less than 1), incompressible theory may be utilized. In this case the Sommerfeld variable must be determined. For convenience, it is generally accepted practice to use the value of the Sommerfeld reciprocal (1/S) where:

$$1/S = \frac{P_{avg}}{\mu N'} \left(\frac{c}{r}\right)^2$$

$$\text{Note, } N' = \frac{\omega}{2\pi} = \frac{N}{60} \text{ rps}$$

$$P_{avg} = \frac{W}{dl} \quad (\text{W} = \text{load capacity, lbs.})$$

If $W' = W/dlP_a$, then 1/S can be reduced to

$$1/S = \frac{12\pi W'}{\Lambda}$$

$$\text{For } \Lambda = 0.44, 1/S = 85.78W'$$

The eccentricity ratio ϵ may be determined for values of load parameter W' and the reciprocal of the Sommerfeld Number (1/S) from Figure 4 reproduced from the design manual. A table of values is listed below:

TABLE I

Values of W and 1/S for l = 1.25" and d = 0.420" ($P_a = 14.7 \text{ psia}$)

<u>ϵ</u>	<u>h_o</u>	<u>1/S</u>	<u>W</u>
0.1	.00018	3.8	.34
0.2	.00016	7.8	.70
0.4	.00012	16.0	1.44
0.6	.00009	26.5	2.38
0.8	.00004	45.5	4.09
0.9	.00002	67.3	6.05

$$h_o = c(1 - \epsilon) \quad (h_o = \text{minimum film thickness})$$

$$1/S = 85.78 W/dlP_a$$

$$W = \frac{1/S}{11.12}$$

A plot of load capacity W versus eccentricity ratio ϵ and minimum film thickness h_o is presented in Figure 5. Utilizing this curve a determination of the rotor operating loads will permit prediction of the minimum film thickness in the bearing.

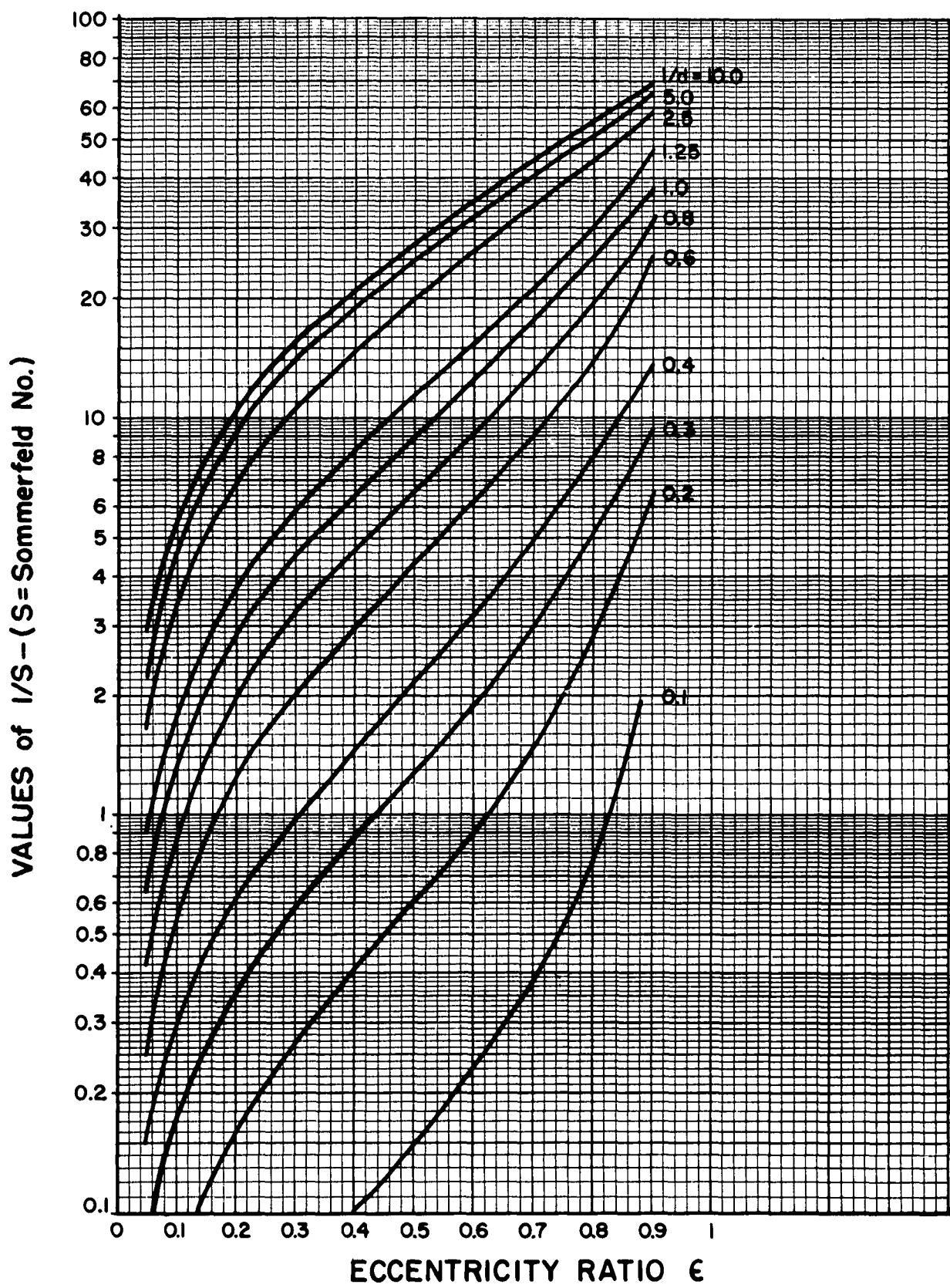


Fig. 4— $1/s$ Plotted Against Eccentricity Ratio for $\Delta \rightarrow 0$

$I/d = 2.98$
 BORE = .420 inch
 LENGTH = 1.250 inches
 RADIAL CLEAR. = .0002 inch
 SPEED = 3300 RPM

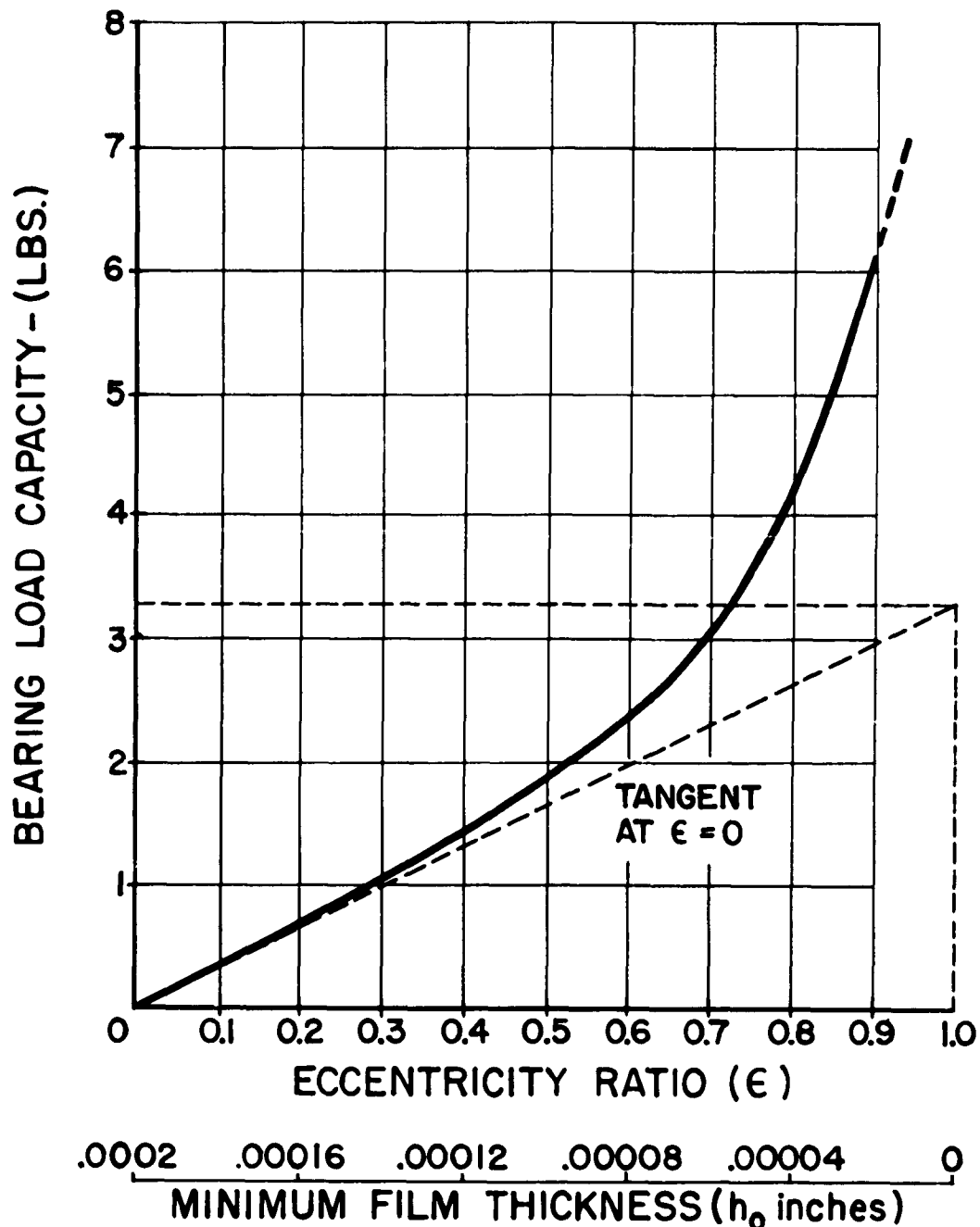


Fig. 5—Bearing Radial Load Capacity
(Plain Journal Bearing)

The three primary loads of concern are:

- a. Rotating unit mass load.
- b. Rotating unbalance loads.
- c. Unbalanced electrical loads.

The rotating unit weight is 0.29 pounds which was determined by weighing the rotating components.

In the case of the unbalance load, a dynamic balance limit of 300 micro ounce inches per balancing plane was selected because of the low speed requirements of the unit. If the locations of unbalance at either end of the rotor are in phase, the total unbalance is 600 micro ounce inches. If the unbalance locations are 180 degrees out of phase, a moment is produced equivalent to the unbalance in one plane times the distance between balancing planes. This condition is considered under moment loads. The maximum radial load can be expressed as

$$F = \frac{wr\omega^2}{g} \text{ lbs.}$$
$$= \frac{.0006 (345.6)^2}{16 \times 386}$$

$$F = 0.0116 \text{ lbs.}$$

The third force of primary concern is that due to magnetic unbalance forces. Magnetic unbalance is the result of an eccentric air gap existing between the motor rotor and stator. An analytical expression was derived by the Rotron Research Corp. for a two pole motor to approximate these forces as follows:

$$F = 17.42 \times \left(\frac{B}{10,000} \right)^2 \times D \times L \times \emptyset$$

where F = force in lbs.

B = Flux Density (lines/in²)

D = Rotor Diameter (inches)

L = Rotor Length (inches)

$$\emptyset = \frac{1}{2r^3} \left(\frac{2-r^2}{2\sqrt{1-r^2}} - 1 \right)$$

$$r = \frac{TIR}{2\Delta} \text{ (dimensionless)}$$

TIR = Radial distance between rotor center and
2 stator center (inches)

Δ = Nominal radial air gap between rotor and
stator (inches)

The force described by this formula is the peak value of a sinusoidal force which oscillates from 0 to F at a frequency of 120 cps for this specific motor. An average value of this peak value is used as the estimated magnetic radial force on the bearing: i.e., F/2. Figure 6 is a plot of the estimated peak radial force due to magnetic air gap eccentricity. The motor design is dimensioned such that the maximum eccentricity is .001 T.I.R. in the air gap region. From Figure 6, this would represent an average magnetic load of 0.325 pounds. The location of this magnetic unbalance force is dependent upon the angular location of the eccentricity. As far as the bearing is concerned, the maximum load would occur when the magnetic force acts in the direction of the gravity force on the rotor.

The summation of the rotor radial forces can be summarized as follows:

a. Rotor weight:	0.290 lbs.
b. Unbalance force at 3300 rpm:	0.0116 lbs.
c. Magnetic unbalance force:	<u>0.325 lbs.</u>

Total Radial Load: 0.6266 lbs.

From Figure 5, this load will result in an eccentricity of 0.21 or a minimum film thickness of .000162 inches. The blower motor, however, must be capable of operating under vibrational loads to 10 g and 55 cps. At this condition the radial load due to rotor mass will increase to 2.9 lbs. with a resultant total load of 3.341 lbs. In this case the eccentricity ratio will increase to 0.72 or a minimum film thickness of .000057 inches.

To estimate the moment carrying capacity of the journal bearing, the analysis of Ausman (Reference 5) is used. Figure 7, reproduced from Ausman's paper, plots a dimensionless parameter H against another dimensionless parameter K where:

$$H = \frac{6\mu\omega}{kP_a} \left(\frac{r}{c}\right)^2$$

$$K = \frac{12 c M}{\pi k P_a r l^3 \delta}$$

k = coefficient of polytropic expansion of gaseous lubricant which for our purposes is isothermal air, therefore, k = 1.0

RANGE STACK HEIGHT: 1.25 in.
AIR GAP FLUX DENSITY: 25,000 lines/in.²
ROTOR DIAMETER : 0.923 in.

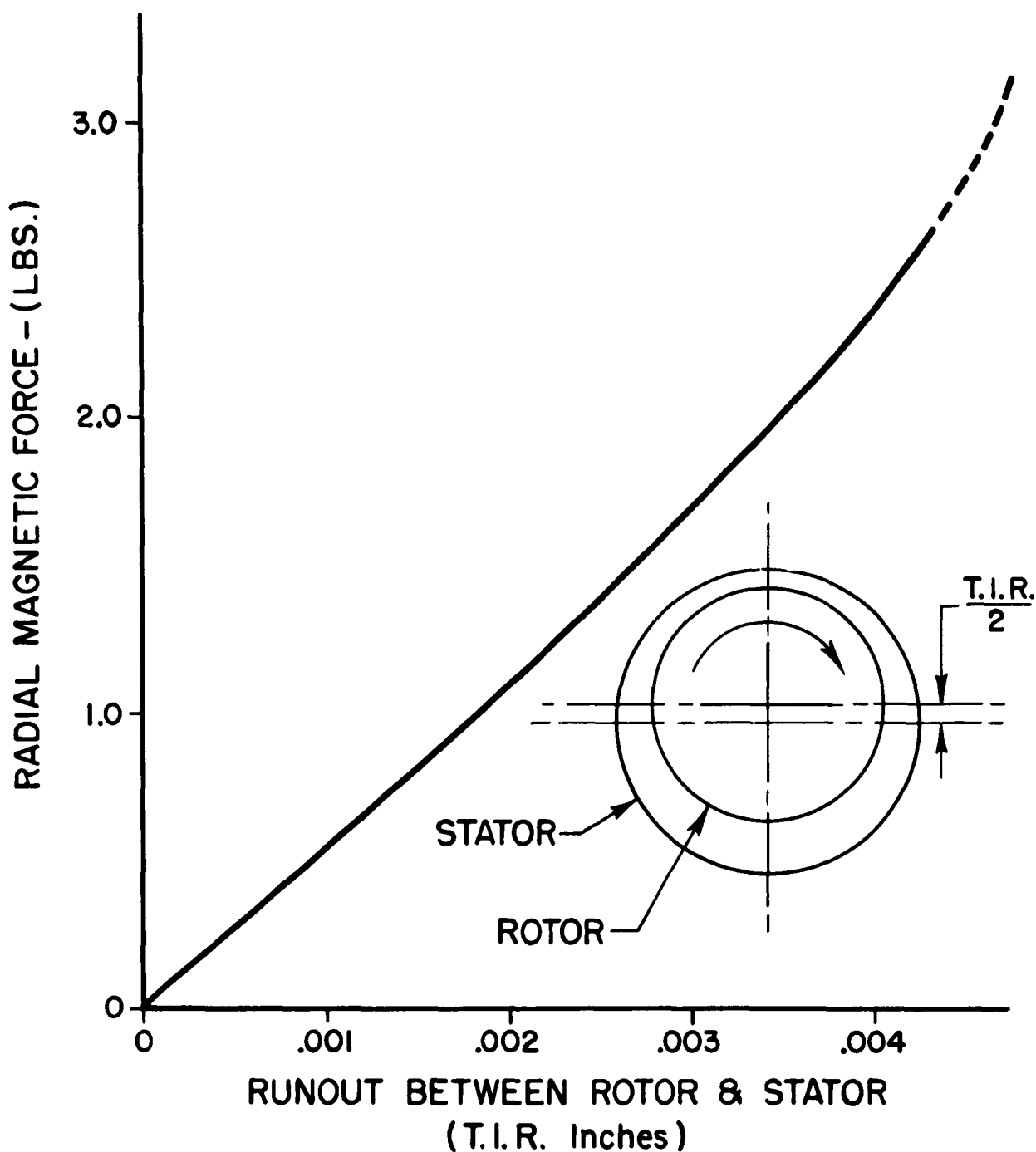


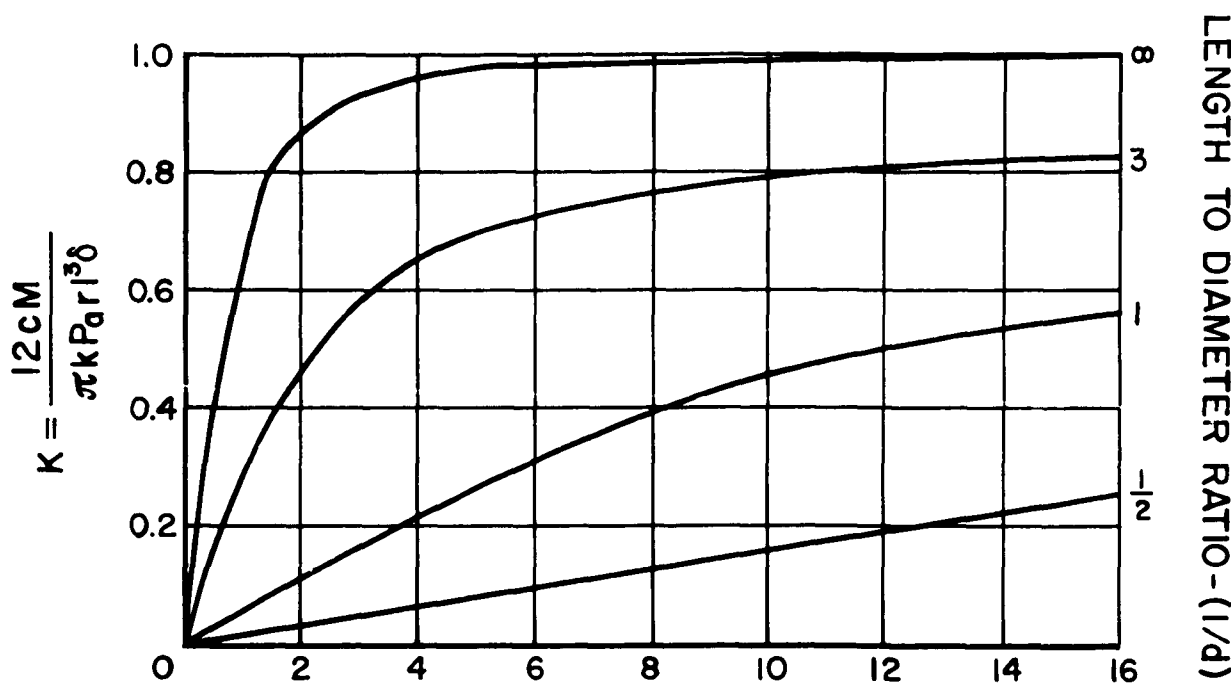
Fig. 6—Induction Motor Magnetic Force

M = moment applied to the bearing (inch pounds)

δ = misalignment angle or angular displacement of journal (radians)

$$H = \frac{6\mu\omega(r)^2}{P_a c} \cdot \frac{1}{k} = \frac{\Lambda}{k} = \frac{.44}{1.0} = .44$$

$$K = \frac{12(.0002) M}{(3.1416)(1.0)(14.7)(.210)(1.25)^3} = 12.68 \frac{M}{\delta} \times 10^{-5}$$



$$H = \frac{6\mu\omega r^2}{k P_a c^2}$$

Fig. 7—Moment Capacity of Full Journal Bearings,
(Ausman, Ref. 5)

From Figure 7

$$K = 0.1335 \text{ for } H = .44 \text{ and } l/d = 3$$

therefore

$$0.1335 = \frac{M}{\delta} (12.68) 10^{-5}$$

$$\delta = 94.9 \times 10^{-5} M$$

The rotor center of gravity is located over the bearing center, therefore, the rotor moment is due to magnetic and unbalance moments as follows:

Maximum Electrical Moment:	0.135 inch pounds
Maximum Unbalance Moment:	<u>0.0127 inch pounds</u>
Total Moment:	0.1477 inch pounds

At a 10 g vibrational load the unbalance moment increases to 0.127 inch pounds resulting in a total moment of 0.262 inch pounds.

Considering the 10 g moment

$$\delta = 94.9 (.262) \times 10^{-5} \text{ radians}$$

$$\delta = 24.85 \times 10^{-5} \text{ radians}$$

$$\tan \delta = \frac{C_{\max}}{1.250}$$

$$C_{\max} = 1.250 (24.8) 10^{-5}$$

$$C_{\max} = .00031$$

$$\text{Minimum clearance} = \frac{C_d - C_{\max}}{2} \quad (C_d = \text{diametral clear.} = .0004 \text{ In.})$$

$$\text{Minimum clearance} = \frac{.0004 - .00031}{2} = .000045''$$

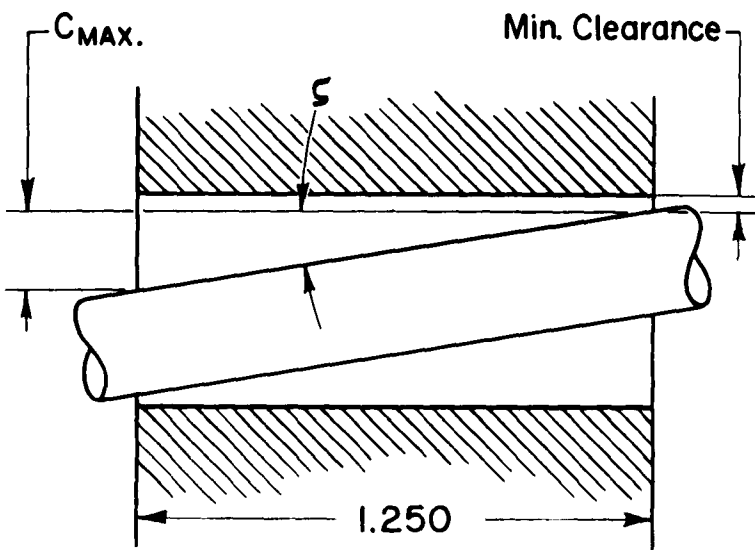


Fig. 8—Maximum Moment Angle δ

One specific type of instability of concern in the bearing, termed synchronous whirl, is the result of rotating unbalance causing the rotor center to describe an orbital path in the rotor clearance at a frequency equal to the rotating frequency of the rotor. The supporting gas film in the bearing can be considered as a spring with a variable spring rate or stiffness under varying load conditions. At increasing rotor speeds, the rotor unbalance force increases until, at the natural frequency of the rotating system, a forced vibration occurs. The natural frequency can be determined from

$$f = \frac{1}{2\pi} \sqrt{\frac{k}{M}}$$

k = film stiffness (lb/in.)

M = total mass of rotating system (W/g lb. sec.²/in.)

f = natural frequency (cycles/sec.)

The film stiffness may be determined from the slope of the load vs. eccentricity curve (Figure 5) at the load condition under consideration. The minimum load will occur with the journal bearing operating in a vertical condition where the mass load due to gravity is zero. If the magnetic load and unbalance load approach zero then the slope may be determined at eccentricity equal to zero. The tangent line is shown on Figure 5.

$$k = \frac{3.3 \text{ lbs.}}{.0002 \text{ in.}}$$

$k = 16,500 \text{ lbs./in.}$

$$f = \frac{1}{2(3.1416)} \sqrt{\frac{16,500}{.29}} \frac{.29}{386}$$

$f = 745.6 \text{ cps}$

Since the unit will operate at 55 cps and vibrational requirements are limited to 55 cps, operation will not approach this critical speed.

B. Test Rig Evaluations

Initial evaluations of the journal bearing were conducted in the test rig described in Reference 29. In order to investigate the effect of electrical loads on the bearing it was necessary to fabricate a second test rig utilizing the motor rotor and stator representative of the final design. This second rig is described under Section IIC "Measurement Procedure" and shown on Figures 1 and 3.

The test rotor for the 29 frame size test rig is sleeved on either end ring outboard of the rotor laminations to provide a sensing area for the capacitive probe pick ups. See Figure 9. The rotating bearing sleeve is inserted in the bore under the center of gravity of the rotor. Because the capacitive probes sense the motion of the outer diameter of the rotor, it is essential that the concentricity between the bearing sleeve and the rotor outer diameter be maintained extremely close. On the test rotors that have been fabricated to date, this concentricity was held to .0001 inches full indicator reading. The capacitive pick up therefore records a sine wave with a peak to peak value of .0001 inches. Utilizing a bearing with a radial clearance of .0002 inches, movements within the bearing of 20 micro inches must be observed to determine bearing characteristics. However, the basic mechanical eccentricity built into the rotor has overshadowed these rotor movements. As a result, two new rotors are presently being fabricated maintaining concentricity of rotor O.D. to bearing bore of 40 micro inches.

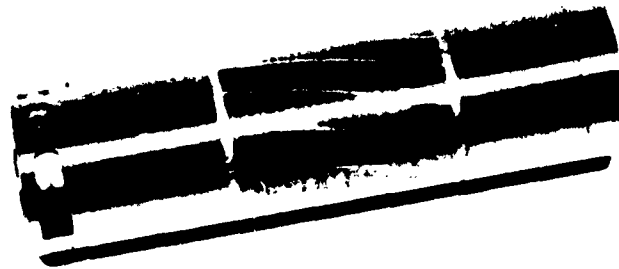


Fig. 9—29 Frame Size Test Rotor

Because of the rotor eccentricities existing during the bearing evaluations conducted to date, additional rig operation is necessary to establish the stable bearing operating range under electrical load conditions. Several observations are apparent from the experiments already conducted. During the rig test phase, the effect of magnetic loads on bearing performance is of interest. Since the angular location of the magnetic load will vary according to the location of the maximum eccentricity between electrical rotor and stator, the electrical

load can oppose or act in phase with the force due to gravity on the rotor. This has been observed in the test rig by rotating the rig 360° on its horizontal axis. When the electrical load is in phase with the mechanical gravity load, the minimum possible supporting film can be observed from the capacitance pick up signal. Because the electrical load is of the same order of magnitude as the weight of the rotating components, it is possible for the electrical load to shift the rotating mass to the center of the bearing clearance. The load capacity of the bearing at this position is zero. Consequently, any small disturbing force would tend to shift the rotor and instabilities of the rotor might occur. Observations, however, have not indicated this type of instability, perhaps due to the difficulty in positioning of the magnetic field to the exact location of opposing magnetic and gravity forces.

C. Gas Bearing Blower Motor

Figure 10 represents the blower motor design being developed for this program. The motor is a 29 frame size lamination (1-13/16" lamination outer diameter) by 1-1/4 inch stack length. The bearing selected for this design is a .420 diameter by 1-1/4 inch long sleeve of ceramic aluminum oxide mounted on a 1/4 inch diameter cantilevered shaft.

In order to reduce the bearing moment loads, the rotating sleeve installed in the rotor is not located directly under rotor laminations but is shifted toward the center of gravity of the rotor. In addition, the rotor center of gravity is shifted over the bearing center by the addition of a steel insert cast into the aluminum rotor end ring. This end also runs in a labyrinth type sealing groove to help maintain the bearing area free of foreign material. Dust shields have been added to either end of the bearing to block further the possibility of debris or dust entering the bearing.

Thrust is absorbed at the blower end of the motor by a molybdenum disulfide impregnated Teflon washer inserted in the blower wheel guide cap running against the crowned end of the hardened steel shaft. Thrust in the reverse direction is absorbed by a lead impregnated, Teflon washer running against a hardened steel washer. These material combinations have shown promise as dry rubbing surfaces in previous evaluations at Rotron under the low speed (3300 rpm) light load conditions of this unit.

During the initial design phase of this blower motor, a .375 diameter bearing was selected for the first development unit. This bearing, however, appeared marginal under bearing moment loading. The bearing size, therefore, was changed to a .420 diameter. The first unit that has just completed fabrication contains a .375 diameter bearing. This unit, as depicted on Figure 11, will be used primarily for thrust bearing evaluations. Two development units containing the .420 diameter bearing are scheduled for completion 12-20-62. Initial operation of these units will be concerned with bearing capabilities under vibratory conditions to 10 g's. Both bearing sizes will contain diametral clearances in the range of .0003 to .0004 inches. Because of the lead time encountered in obtaining ceramic parts, the first development units will contain

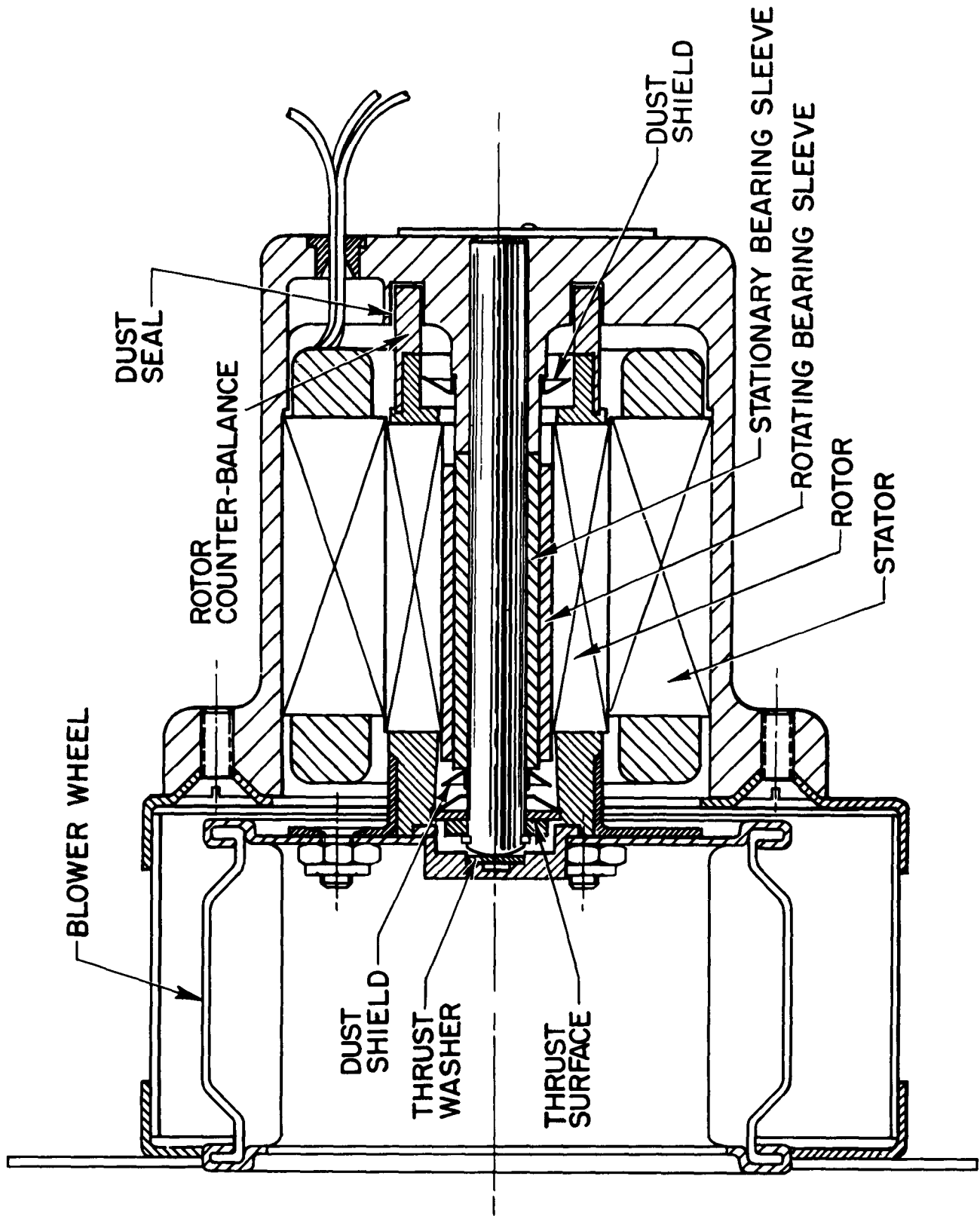


Fig. 10—29 Frame Blower Motor Design

416 stainless steel electrolized coated bearing sleeves. Later evaluations will include aluminum oxide ceramic as the journal bearing material.

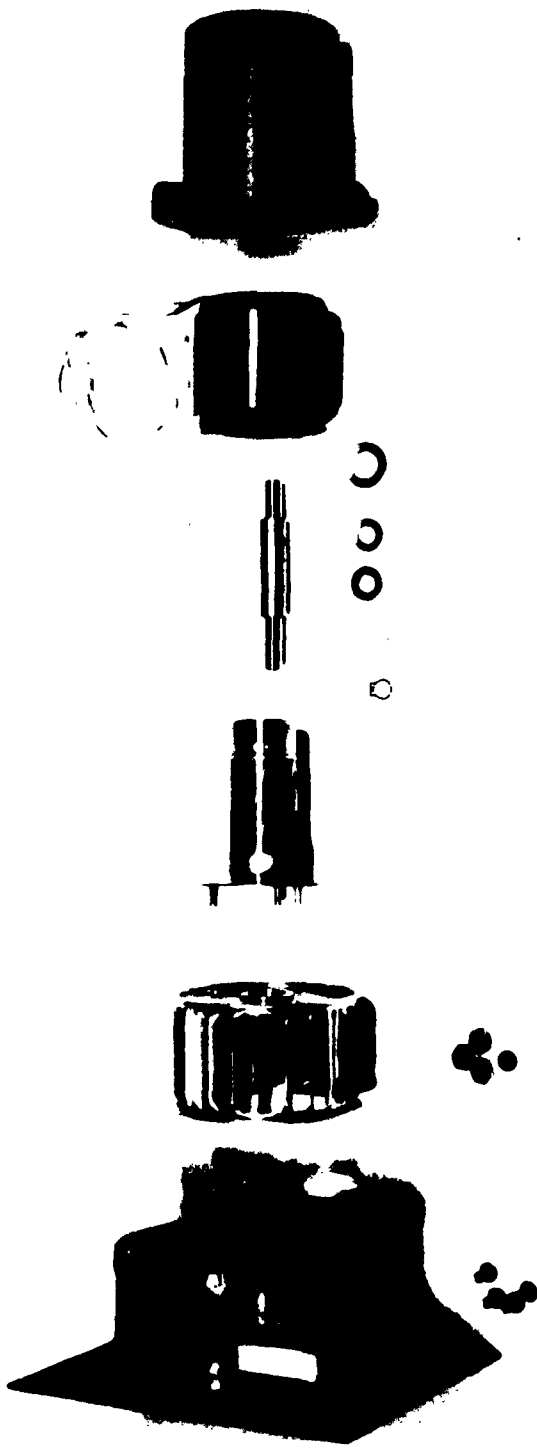


Fig. 11—First Development Prototype Unit

The first motor rotor casting and stator winding assembly was evaluated on a dynamometer utilizing a dummy housing to check motor performance. The resultant characteristics are presented on Figure 12 and are within the calculated values.

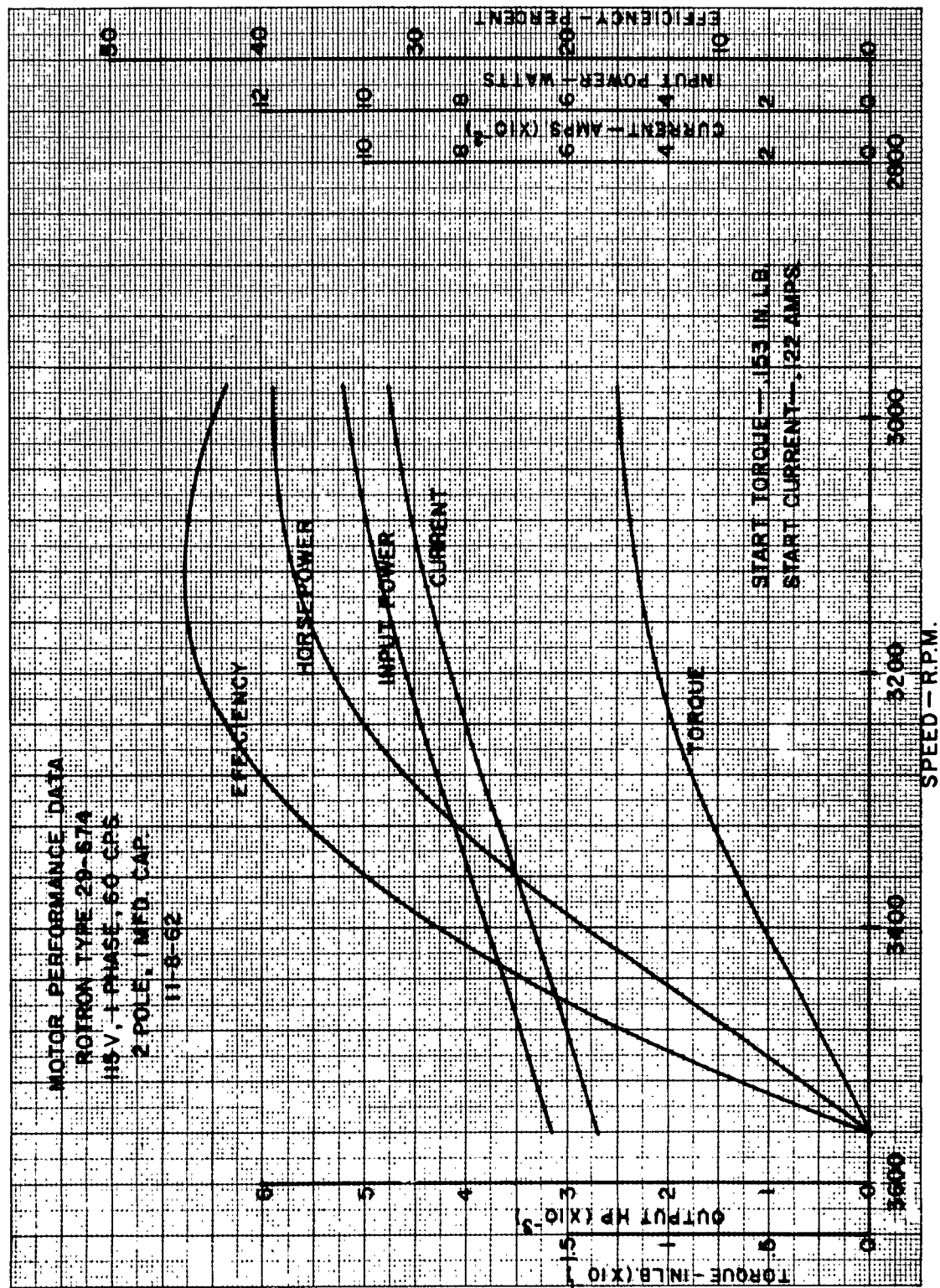


Fig. 12—29 Frame Motor Performance

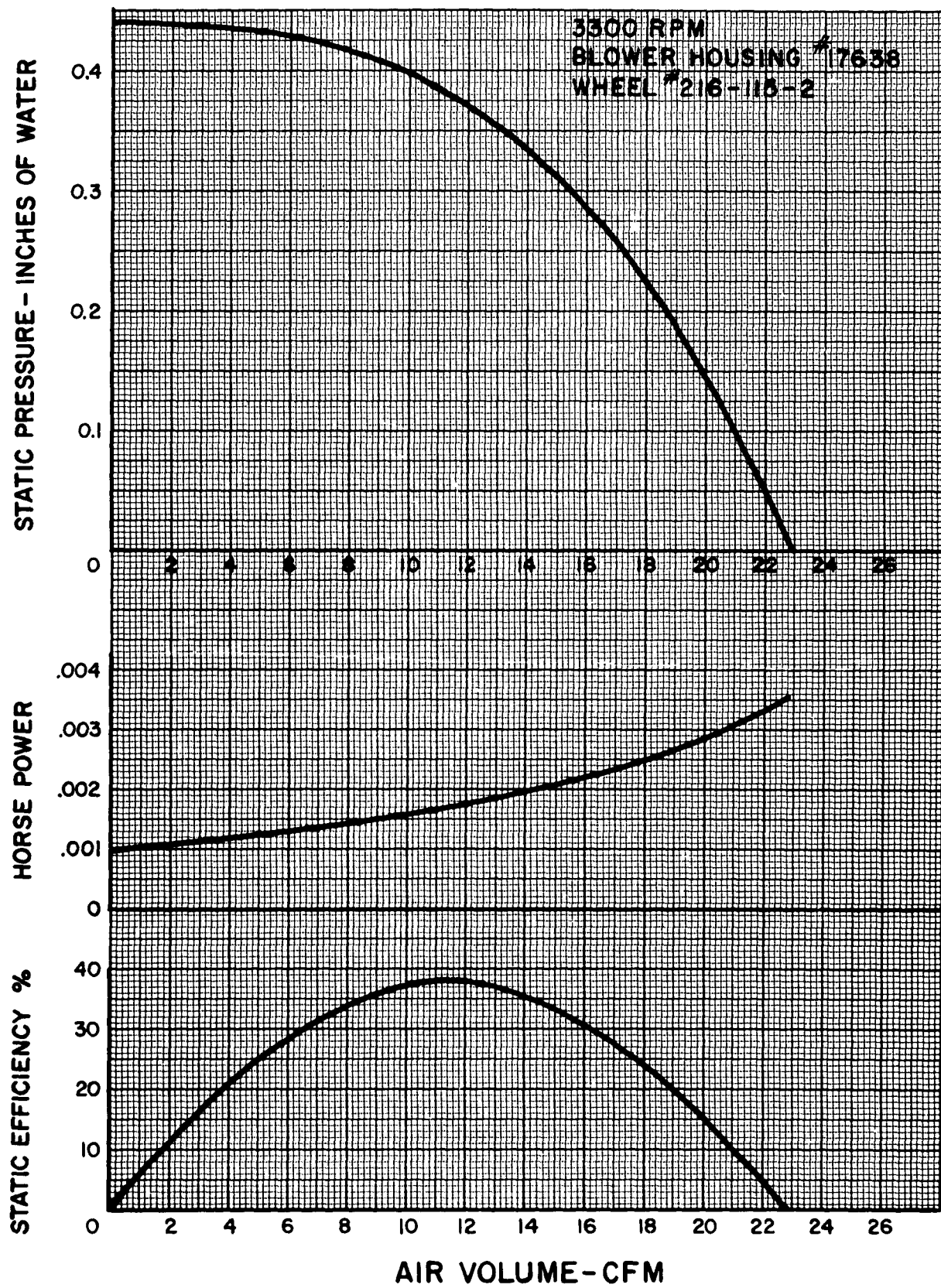


Fig. 13—Blower Aerodynamic Performance

A motor impeller housing was fabricated in accordance with Bureau of Ships Drawing RE-46C 2105. A Torrington type 216-115-2 centrifugal fan was evaluated in the housing on a dynamometer at 3300 rpm to determine blower characteristics. The results of this evaluation are presented on Figure 13, which shows the maximum motor load requirement to be .0032 HP. From Figure 11, the motor speed range will be 3380 to 3490 rpm with an input power requirement of 7.7 to 6.8 watts.

The motor design was based on the power requirements of the specified blower wheel in a standard housing. The modified blower housing specified on the BuShips drawing reduced the wheel characteristics and thus the motor load requirements. A reduction in motor input and output power is possible in view of the reduced wheel power requirements. However, this would also produce a reduction in the motor starting torque. It is desirable to maintain the higher starting torque characteristics to insure sufficient power to drive the dry bearing running sleeves until the bearing becomes airborne. No modifications, therefore, are being considered to the motor design at this time.

D. Project Performance and Schedule

The project Schedule is outlined on Figure 14 from program inception to December 7, 1962, shown as solid bars. Symbols used on Figure 13 are explained on the following page where an estimation of the percentage of total program effort expended to date may also be found.

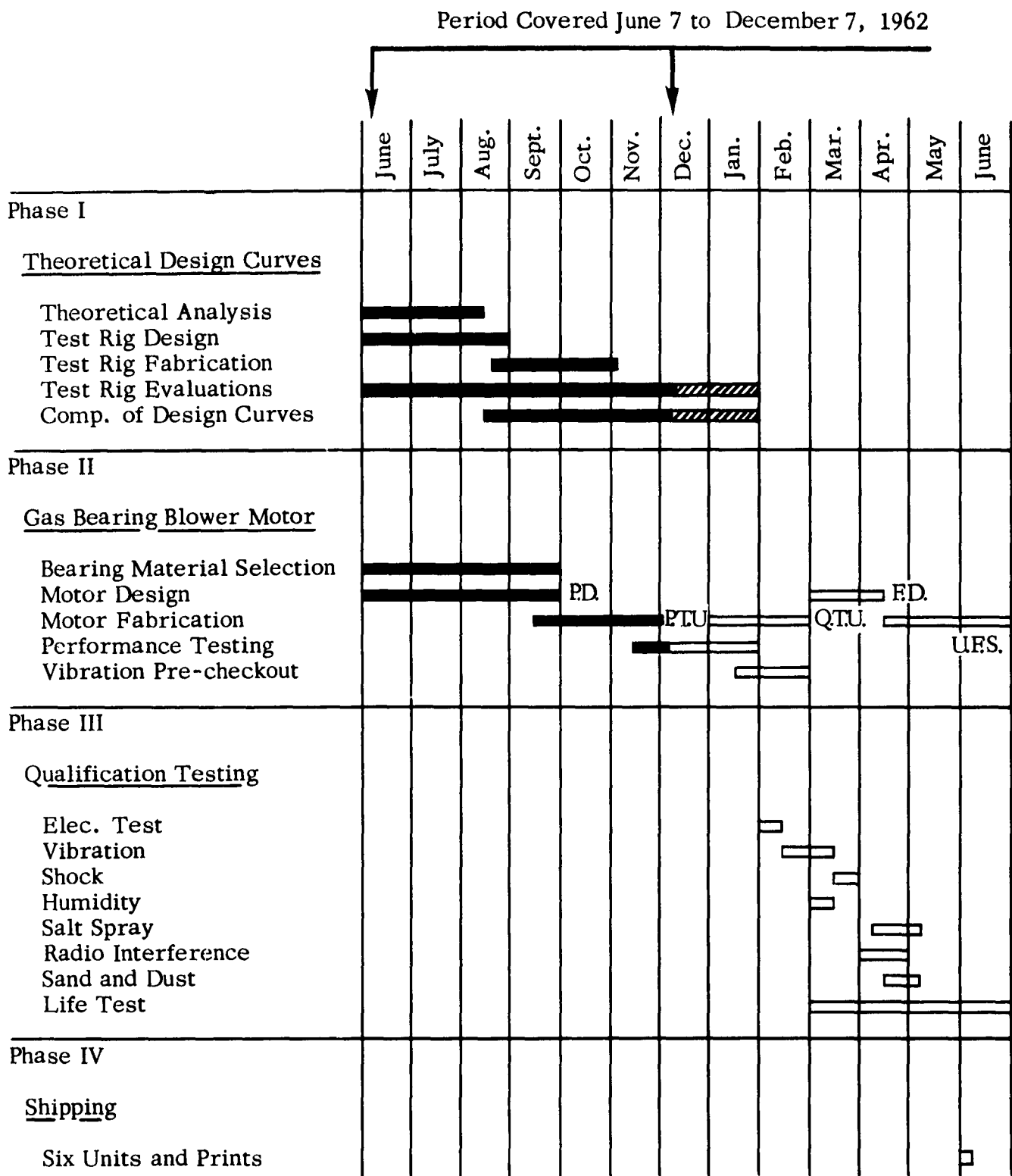


Fig. 14—Project Performance and Schedule
Rotron Manufacturing Co., Inc.
Contract No. NObsr-87522

ROTRON MANUFACTURING COMPANY
PROJECT AND PERFORMANCE SCHEDULE

Legend	Description
	Work Performed
	Schedule of Projected Operation
	Revised Schedule of Projected Operation
P. D.	Preliminary Drawings
F. D.	Final Drawings
P. T. U.	Performance Test Units
Q. T. U.	Qualification Test Units
U. F. S.	Units for Shipment

Estimated completion in percent of Total Effort expected to be expended

1. Initial Theoretical Analysis	100%
2. Test Rig Design and Fabrication	100%
3. Test Rig Evaluations	40%
4. Gas Bearing Design Manual	75%
5. Gas Bearing Blower Motor	50%
6. Qualification Testing	0%

Notes

Test rig evaluations have been extended from 11/31/62 to 1/31/63. The completion of design curves has been extended from 12/31/62 to 1/31/63. All remaining phases of the program are on schedule.

CONCLUSIONS

The theoretical design analysis has been completed on the .420 diameter by 1.250 long plain journal bearing to be utilized in the 29 frame size gas bearing blower motor. A bearing diametral clearance range of .0003 to .0004 inches will be utilized in this bearing resulting in a minimum film thickness of .000162 inches under normal operation and .000057 inches under 10 g vibrational load. Moment load capabilities under 10 g vibration loads are well within the bearing capabilities. The natural frequency of the bearing is 745 cps, which is well above the maximum operating speed, thereby insuring operation outside the region of synchronous resonant whirl.

Design of the gas bearing blower motor has been completed and the first prototype has been fabricated. The motor performance testing and blower performance testing have demonstrated the capabilities of the design in meeting the performance characteristic requirements of MIL-B-21399A.

A. Future Work

1. Completion of the Gas Bearing Design Manual.
2. Continuation of rig evaluations to determine the stability effects of magnetic loading.
3. Development evaluations of the gas bearing blower.